

Influence of Interstitial Impurities (H, B, C) on Grain Boundary Cohesion in B2 Ti-based Alloys

S.E. Kulkova^{1,2,*}, A.V. Bakulin^{1,†}, S.S. Kulkov², S. Hocker³, S. Schmauder³

¹ Institute of Strength Physics and Materials Science of Siberian Branch Russian Academy of Science, 2/4, Akademicheskoy pr., 634021 Tomsk, Russia

² National Research Tomsk State University, 36, Lenina pr., 634050 Tomsk, Russia

³ Institute of Materials Testing, Materials Science and Strength of Materials, University of Stuttgart, 32, Pfaffenwaldring str., D-70569 Stuttgart, Germany

(Received 29 June 2013; published online 03 September 2013)

The investigation of hydrogen, boron and carbon sorption properties at the $\Sigma 5(310)$ symmetrical tilt grain boundary (*GB*) and (310) free surface (*FS*) in B2 Ti-based alloys was carried out by the plane-wave pseudopotential method within density functional theory. The most preferential positions for interstitial impurities at *GB* were determined. It was shown that impurities sorption energies at *GB* depend strongly on their local environment. The analysis of electronic properties allows us to establish the microscopic nature of chemical bonding of all considered impurities at *GB*. It was shown that H decreases more significantly the surface energies than the *GB* energy in contrast to B and C. This results in decreasing the Griffith work that indicates also the decrease of the strength of grain boundary. The segregation of H at the *GB* makes intergranular fracture much easier because the bonding between metal atoms, which are neighbors of H, is weakened. The segregation behavior of hydrogen confirms it as an embrittler for B2 Ti-based alloys. At the same time boron and carbon segregation contrast to hydrogen increase the *GB* cohesion.

Keywords: Absorption/adsorption, Impurities, Hydrogen, electronic structure, Grain boundaries, Surface, Griffith work.

PACS numbers: 68.35.Dv, 68.35.Np, 68.43.Bc, 68.43.Fg, 68.47.De, 71.15.Mb

1. INTRODUCTION

The behavior of hydrogen in metals has been extensively studied over the last century [1]. Interest to hydrogen is caused by possibility of its usage as an alternative ecological and clean energy source. The most attractive and safe method among chemical ones is the storage of hydrogen in the form of metal hydrides or in hydrides of intermetallic compounds. Hydrogen storage elements on the base of metals, which have a high affinity to hydrogen, are used in practice already [2]. At the same time hydrogen influences considerably the mechanical properties of materials. Even low concentrations of hydrogen can affect considerably the mechanical strength of transition metals and alloys, since they become brittle. This phenomenon called “hydrogen embrittlement” (HE) may limit industrial applications of functional materials. In spite of attempts to explain the mechanism of HE [3-5], its microscopic origin remains unclear up to now. Intermetallic alloy TiFe is known as the best candidate for hydrogen storage since it may form hydrides at the atmospheric pressure and room temperature. Its main drawback is the difficulty in the activation treatment. During this process the surface oxide layer, which hinders hydrogen sorption, can be formed. It was shown that the use of a palladium coating may prevent the formation of surface oxide films on TiFe [3, 4], moreover as was shown in our previous papers [5,6] hydrogen can penetrate in bulk material with Pd coating. Alloying by other metals as well as the usage of nanostructural alloys also improved hydrogen storage properties.

For better understanding of the behavior of H in materials and its effect on their physical and mechanical properties, the real polycrystalline structure of materials should be taken into account. Grain boundaries are among the most important internal interfaces in crystals that can degrade their mechanical properties. In polycrystalline materials, impurities may diffuse along *GB* and segregate at them. As a result, hydrogen accumulates at *GB* and can stimulate fracture along them. At the same time other interstitial impurities such as boron may increase *GB* cohesion as was shown in [7]. Grain boundary diffusion controls the kinetics of many microstructural changes, phase transformations, and other important processes in materials that are critical for their production and application [8]. *Ab initio* methods within density functional theory (DFT) can be useful tools to understand the microscopic mechanisms of hydrogen sorption on internal and external interfaces, to calculate the characteristics that quantitatively determine the energy required to divide a crystal along tilt grain boundaries, and to reveal the role of hydrogen in brittle fracture.

Main goal of this work is to study the effect of some interstitial impurities (H, B, C) on *GB* cohesion in binary TiMe alloys with $Me = Fe, Co, Ni$.

2. COMPUTATIONAL DETAILS

For *GB* simulation in the metallic systems the embedded atom method (EAM) is widely used but its accuracy is limited in comparison with an *ab initio* approach since the interatomic potential parameters are determined in this

* kulkova@ispms.tsc.ru

† bakulin@ispms.tsc.ru

method by means of empirical data. In contrast to empirical methods, the first-principles methods based on the DFT are applicable to wider range of the metallic systems and allow performing fully relaxed total energy calculations. The accurate total energies need for correct determination of the impurity binding, sorption and segregation energies at *GB* and surface. The calculation of the atomic and electronic structure of binary Ti-based alloys with symmetrical tilt grain boundary $\Sigma 5(310)$ and (310) free surface was carried out by the plane-wave pseudopotential method implemented in the VASP code [9, 10] with the generalized gradient approximations (GGA) of Perdew et al. (PW91) [11] for the exchange-correlation functional. The *GB* and *FS* calculations were performed using supercell approach with periodic boundary conditions. In order to describe *B2-TiMe* alloy with $\Sigma 5(310)$ *GB* and (310) stepped surface we used unit cells consisting of 40 and 22 atoms, respectively. In this case *GB* supercell has orthorhombic symmetry with lattice parameters of $a_0\sqrt{10}$, a_0 , $a_0 2\sqrt{10}$. There was 20 atom layers structure and each layer contained both Ti and *Me* atoms, and two identical grain boundaries were introduced. The *TiMe*(310) surface was simulated by a slab model with ten layers of Ti and *Me* and vacuum between slabs. Note that the slab contains two different surfaces in this case. The relaxation of atomic positions was performed in the direction perpendicular to *GB* (*FS*) as well as in the planar directions. The optimization of shape and atomic positions were carried out in case of *GB* whereas the lattice parameters of two dimensional unit cell were fixed in the calculations of the (310) surface. Each system with *GB* or *FS* was fully relaxed by minimizing forces on atoms to less than 0.02 eV/Å. The total energy tolerance was set at 1×10^{-5} eV/atom. The cutoff energy of plane waves was set at 350 eV. The $16 \times 16 \times 16$ *k*-point grid was used in the bulk calculations but $4 \times 9 \times 2$ ($4 \times 9 \times 1$) grids of *k*-points were used in case of *GB* (*FS*), respectively. It should be noted that the relaxation effect was expressed significantly near the *GB* plane and in the surface layers. The binding (E_b) and absorption/adsorption ($E_{abs/ads}$) energies can be defined in the same manner, as given in Eqs. (1, 2):

$$E_b = -1 / 2 \times (E_{H-TiMe} - E_{TiMe} - 2 \times E_H) \quad (1)$$

$$E_{abs/ads} = -1 / 2 \times (E_{H-TiMe} - E_{TiMe} - E_{H_2}) \quad (2)$$

In these equations E_{H-TiMe} and E_{TiMe} are the total energies of systems with and without hydrogen, E_H

and E_{H_2} are the energies of hydrogen atom and molecule, respectively.

3. RESULTS AND DISCUSSION

Fig. 1 presents the atomic structure of the *B2-TiMe* alloy with $\Sigma 5(310)$ *GB*. There are two types of *GB* holes with different compositions which can be occupied by impurity atoms. It is seen from Fig. 1 there are two triangles (large and small) formed by *Me* or Ti atoms at the *GB*, where, for example, H atom was initially positioned. Two positions of hydrogen atom (H1 and H2) in Fig. 1 are located in the plane which cuts the *Me* *GB* atoms and other two positions (H3 and H4) are in the second plane which cuts the Ti *GB* atoms, respectively. Similarly to the *GB*, there are also two types of surface holes in the case of the *TiMe*(310) surface. It is well known that in the bulk *B2-TiMe* alloys hydrogen can occupy two different octahedral sites which are distinguished by their composition. At the first type of octahedral sites the H atom is surrounded by four Ti atoms and two *Me* atoms whereas at the second type of octahedral positions it has four *Me* and two Ti atoms as first neighbors. One of the atom of *Me* or Ti is absent at $\Sigma 5(310)$ *GB* in case of H1 or H3 sites.

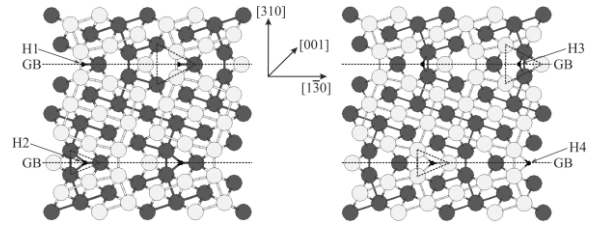


Fig. 1 – Atomic structures of *TiMe* alloy with a symmetric $\Sigma 5(310)$ tilt grain boundary and hydrogen located in the following four sorption positions: H1 and H2, at the centers of the large and small metal triangles, respectively; H3 and H4, at the centers of the large and small titanium triangles, respectively. Atoms *Me*, Ti, and H are given by large dark, large bright, and small dark balls, respectively. Grain boundaries are shown by dashed lines.

The calculated hydrogen absorption energies in the four positions in the *TiMe* $\Sigma 5(310)$ are given in Table 1. It is seen that at *GB* the hydrogen absorption energies in positions H1, H2, and H4 decrease slightly in case of *TiFe* but they are almost the same for *TiCo* and *TiNi*. Actually the absorption energy weakly depends on a second alloy component.

Table 1 – Absorption/adsorption energies of H (in eV) and bond lengths d (in Å) at the *TiMe* $\Sigma 5(310)$ *GB* and on the *TiMe*(310) *FS*.

H-position	E_{abs}			$d(H-Me)/d(H-Ti)$		
	TiFe	TiCo	TiNi	TiFe	TiCo	TiNi
H1	0.32	0.31	0.35	1.61 (2.01)	1.73 (1.99)	1.73 (1.97)
H2	0.30	0.36	0.37	1.76-1.77 (2.46)	1.73 (2.08)	1.69-2.25 (2.18)
H3	0.28	0.10	0.08	1.89 (2.07)	1.89 (2.10)	1.94 (2.16)
H4	0.06	0.32	0.35	2.72 (1.72-1.74)	2.82-3.09 (1.77)	2.75 (1.75-1.78)
H-position	E_{ads}			$d(H-Me)/d(H-Ti)$		
	TiFe	TiCo	TiNi	TiFe	TiCo	TiNi
H1	0.91	0.72	0.64	1.62 (2.01)	1.72 (2.02)	1.70 (2.01)
H2	0.80	0.57	0.43	1.66-1.77 (2.21)	1.67-1.82 (2.12)	1.68-1.77 (2.09)
H3	0.72	0.46	0.35	1.80 (2.13)	1.76 (2.15)	1.74 (2.15)
H4	0.37	0.73	0.66	3.13 (1.90-1.91)	3.14 (1.88-1.89)	3.09 (1.86)

Our calculations show that hydrogen absorption is unfavorable in the H3-position, which is enriched by a metal. Similar behavior of the sorption characteristics was observed in our earlier work [12] where the adsorption of H was considered in the hollow position on the metal terminated TiMe(001) surface. Note that the H3-position is similar to the hollow surface position in the local environment of hydrogen. Moreover, the authors of [13] also emphasized that the tetrahedral positions in metal rich clusters become less favorable for hydrogen sorption in binary titanium alloys when the metal bond becomes stronger. Note that the neutron diffraction study of the TiFe alloy showed predominant accumulation of deuterium on grain boundaries in titanium rich positions [14]. The adsorption energies in the series of alloys under study are also given in Table 1. In general, the hydrogen sorption energies on the TiMe(310) surfaces are higher than those at GB; that is, hydrogen prefers to be adsorbed on a free surface. Note that the adsorption energy on the TiFe(310) surface reaches maximal value (0.91 eV) for the H1-position. In addition, our calculations reveal that the change in the sorption energy in TiFe as a function of a H position is similar on both interfaces. In case of TiCo and TiNi alloys, the adsorption energy in the H1-position is insignificantly lower than in the H4-position, which corresponds to the bridge position between two Ti atoms. As seen from Table 1 adsorption energies in the H3-position are substantially lower in case of TiCo and TiNi alloys. Our calculations showed that the titanium rich positions on the TiMe(310) surface, as those on the TiMe(001) and (110) surfaces, are more preferred for the adsorption of atomic hydrogen for alloys under study.

Griffith work (GW) is a characteristic directly related to fracture. In order to demonstrate the effect of impurity on Griffith work due to their segregation in alloy surface or at GB , the calculation of a number of energy characteristics, such as the grain boundary (E_{GB}) and surface (E_{FS}) energies and their changes during hydrogen sorption were performed. In this case we follow to denotations introduced in the paper [7]. The grain boundary energy of an alloy is the difference between the total energy of an N atomic cell with two tilt grain boundaries ($E_{GB}(N)$) and the energy of the cell containing the same number of atoms in the bulk environment ($E(N)$), i.e., without GB .

Table 2 – Segregation energies of interstitial impurities in the H1-position at the grain boundary and in the corresponding position on a free surface as well as the change of the Griffith work due to impurity segregation (in J/m^2)

I -position	E_{GB}^I	E_{GB}	ΔE_{GB}^I	$E_{FS}^I + E_{FS}$	$2E_{FS}$	ΔE_{FS}^I	E_{GW}	E_{GW}^I	ΔE_{GW}^I
H-TiFe	1.38	1.61	-0.23	5.27	5.86	-0.59	4.25	3.89	-0.36
H-TiCo	0.73	0.64	0.09	4.42	4.66	-0.24	4.02	3.69	-0.32
H-TiNi	0.34	0.18	0.16	4.07	4.14	-0.07	3.96	3.73	-0.23
B-TiFe	0.15	1.61	-1.47	5.29	5.86	-0.58	4.25	5.14	0.89
B-TiCo	-0.09	0.64	-0.73	4.42	4.66	-0.24	4.02	4.51	0.49
B-TiNi	-0.34	0.18	-0.52	3.98	4.14	-0.16	3.96	4.32	0.36
C-TiFe	0.69	1.61	-0.92	5.37	5.86	-0.50	4.25	4.67	0.42
C-TiCo	0.35	0.64	-0.29	4.44	4.66	-0.21	4.02	4.10	0.08
C-TiNi	0.050	0.18	-0.13	3.92	4.14	-0.22	3.96	3.87	-0.09

All calculated energetic characteristics are given in the Table 2. It is seen that for hydrogen at H1-site in TiFe, both GB and FS segregation energies are negative that means the possibility of H segregates to surface and GB as well. It should be noted that for H at H4-site, we get a

$$E_{GB} = -\frac{1}{2S}[E(N, 2GB) - E(N)] \quad (3)$$

For an alloy with an impurity atom in the interstitial positions at an interface, we use the following formula:

$$E_{GB}^I = \frac{1}{2S}[E(N + 2I, 2GB) - E(N + 2I)], \quad (4)$$

here S is the GB plane area. Since our model contains two symmetric tilt grain boundaries, this is reflected by factor 2. The impurity segregation energy at an interface is

$$E_{GB}^I = \frac{1}{2S} \{ [E(N + 2I, 2GB) + E(N)] - [E(N + 2I) + E(N, 2GB)] \} \quad (5)$$

The equations for calculating the surface energy of the alloy with impurity atom (E_{FS}^I) and without it (E_{FS}) and the energy of impurity segregation on the surface (ΔE_{FS}^I) are the same as in [7]. The Griffith work can be calculated in case of impurity undoped and doped system using equations:

$$E_{GW} = 2E_{FS} - E_{GB} \quad (6)$$

$$E_{GW}^I = E_{FS}^I + E_{FS} - E_{GB}^I, \quad (7)$$

where E_{GW}^I , E_{GB}^I and E_{FS}^I are the Griffith work, grain boundary and surface energies for impurity doped system, respectively. The influence of interstitial impurities on the Griffith work can be evaluated by comparing the Griffith work of the systems with and without impurity atom:

$$\Delta E_{GW}^I = E_{GW}^I - E_{GW}. \quad (8)$$

Finally, the change of the Griffith work due to impurity segregation can be calculated as the difference in GW for impurity doped and undoped systems or the difference between segregation energies of the impurity to surface and GB

$$\Delta E_{GW}^I = \Delta E_{FS}^I - \Delta E_{GB}^I. \quad (9)$$

smaller in magnitude value of GB segregation energy (-0.09 eV) which means that H much weakly segregates to this site in comparison with H1-site. It is seen from Table 2, H decreases more Griffith work (negative value of ΔE_{GW}^I) that indicates also significantly the surface ener-

gies than the grain boundary energy, which results in decreasing the the decrease of the strength of grain boundary. The similar trend was obtained for all considered positions of hydrogen as well as for hydrogen sorption in case of TiCo and TiNi alloys. The change of Griffith work in case of TiFe is -0.21 eV for H4-position. It necessary to point out that the values obtained using ten-layers model for surface differ only slightly of ~ 0.05 eV from those obtained with symmetrical 11-layer model.

The analysis of electron characteristics such as electron densities of states (DOS) and charge density distribution allows us to establish the changes in the local DOS of interfacial atoms. It was shown that H interacting with metal atoms induces small peaks at the corresponding local DOS of metal atoms at the same energy region of its valence band. In general, the states of GB atoms involved in the interaction with H, change significantly only. The introduction of H in a metal matrix is known to weaken interatomic bonds. This behavior is also observed at GB. For example, the maximum effect in TiNi is observed when H is incorporated into positions H1 and H4. In this case, the interatomic distances between grain boundary Ti atoms increase by about 0.2 Å and those between Ni atoms only by 0.03 Å.

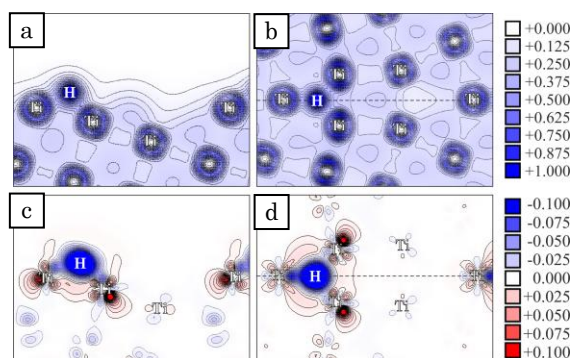


Fig. 2 – Total charge density distributions at FS (a) and GB (b) and difference of the charge densities $\Delta\rho$ in the plane passing through titanium atoms and normal to the interfaces (c) and (d) for H sorption in H4-position at TiNi $\Sigma 5(310)$ and TiNi(310) surface. The isoline spacing is 0.04 el./Å³ in the top pictures and 0.008 el./Å³ in the bottom ones. Negative and positive values of $\Delta\rho$ are shown by dotted and solid lines, respectively.

Note that the effect of weakening the Ni–Ni bond is also rather weak when H is incorporated into distorted octahedral H3-position enriched by nickel. The interatomic distance between Ni atoms increases only by 0.05 Å. As seen from Fig. 2 the hybridization of the orbitals of H and

Ti GB atoms weakens the interaction between Ti atoms. The regions with negative values of $\Delta\rho$ correspond to the accumulation of an electron charge. It is seen that a small charge accumulates near hydrogen but a region with a positive charge density is observed between titanium atoms at GB. Note also that the interatomic bond weakening effect is more pronounced in the TiFe and TiCo alloys. It is known that the surface has a larger number of H sorption positions as compared to GB. Moreover, the situation when hydrogen is located on a free surface is energetically favorable. Therefore, hydrogen accumulation at grain boundaries can favor brittle fracture of a material along an interface with the formation of two free surfaces.

Other impurities such B or C in contrast to H lead to opposite effect on the Griffith work. It is seen from Table 2 that boron prefers to segregate towards GB rather than FS. Such behavior of B leads to positive value of ΔE_{GW}^I in Ti-based alloys similarly to Ni₃Al [7]. In case of carbon this effect is more pronounced for TiFe. In case of TiNi the calculated value of ΔE_{GW}^I for carbon in the H1-position is slightly negative but the values of 1.06, 0.44 and 0.14 eV were calculated for the H2, H3, and H4 positions, respectively.

4. CONCLUSION

The effect of interstitial impurities (H, B, C) segregation on the Griffith work was studied by *ab-initio* approach within DFT. The calculated energy characteristics demonstrate that hydrogen affects the surface energy more substantially than the grain boundary energy. This behavior of hydrogen leads to a decrease in Griffith work and can promote fracture along grain boundaries. It is shown that a boron or carbon impurities in titanium alloys is favored an enhancement of Griffith work and the chemical bond on grain boundaries.

ACKNOWLEDGEMENTS

Numerical calculations were performed on the SKIF-Cyberia supercomputer at National Research Tomsk State University. The reported study was partially supported by DFG research project Schm 746/133-1 and stipendium of President of the Russian Federation for postgraduate student (A.V.B). The work is done partially under the project 2.3684.2011 of Tomsk State University and project ISPMS SB RAS III.23.1.1.

REFERENCES

1. *Hydrogen in Metals* (Ed. G. Alefeld, J. Völkl) (Heidelberg: Springer: 1978, Moscow: Mir: 1981).
2. V. Guthier, A. Otto, *J. Alloys Compd.* **293–295**, 889 (1999).
3. E.M.B. Heller, J.F. Suyver, A.M. Vredenberg, D.O. Boerna, *Appl. Surf. Sci.* **150**, 227 (1999).
4. J. Sanders, B. Tatarchuk, *J. Phys. F: Met. Phys.* **18**, L267 (1988).
5. J.S. Kim, S.Y. Oh, G. Lee, Y.M. Koo, S.E. Kulkova, V.E. Egorushkin, *Int. J. Hydrogen Energy* **29**, 87 (2004).
6. S.E. Kulkova, S.V. Eremeev, V.E. Egorushkin, J.S. Kim, S.Y. Oh, *Solid State Commun.* **126**, 405 (2003).
7. Q.M. Hu, R. Yang, D.S. Xu, Y.L. Hao, D. Li, W.T. Wu, *Phys. Rev. B: Condens. Matter* **67**, 224203 (2003).
8. D. Gupta, *Interface Sci.* **11**, 7 (2003).
9. G. Kresse, J. Hafner, *Phys. Rev. B* **47**, 558 (1993).
10. G. Kresse, J. Furthmuller, *Comp. Mater. Sci.* **6**, 15 (1996).
11. J.P. Perdew, K. Burke, M. Ernzerhof, *Phys. Rev. Lett.* **77**, 3865 (1996).
12. S.S. Kul'kov, S.V. Eremeev, S.E. Kul'kova, *Phys. Solid State* **51**, 1281 (2009).
13. H. Yukawa, K. Nakatsuka, M. Morinaga, *Sol. Energy Mater. Sol. Cells* **62**, 75 (2000).
14. K. Itoh, H. Sasaki, H.T. Takeshita, K. Mori, T. Fukunaga, *J. Alloys Compd.* **404–406**, 95 (2005).